



Aaij, R. et al. (2013) Measurement of the D^\pm production asymmetry in 7 TeV pp collisions. *Physics Letters B*, 718 (3). pp. 902-909. ISSN 0370-2693

Copyright © 2012 CERN, for the benefit of the LHCb collaboration

<http://eprints.gla.ac.uk/80187/>

Deposited on: 3 June 2013

Enlighten – Research publications by members of the University of Glasgow
<http://eprints.gla.ac.uk>



Measurement of the D^\pm production asymmetry in 7 TeV pp collisions [☆]

LHCb Collaboration

ARTICLE INFO

Article history:

Received 16 October 2012

Accepted 12 November 2012

Available online 19 November 2012

Editor: L. Rolandi

ABSTRACT

The asymmetry in the production cross-section σ of D^\pm mesons,

$$A_P = \frac{\sigma(D^+) - \sigma(D^-)}{\sigma(D^+) + \sigma(D^-)},$$

is measured in bins of pseudorapidity η and transverse momentum p_T within the acceptance of the LHCb detector. The result is obtained with a sample of $D^+ \rightarrow K_S^0 \pi^+$ decays corresponding to an integrated luminosity of 1.0 fb^{-1} , collected in pp collisions at a centre of mass energy of 7 TeV at the Large Hadron Collider. When integrated over the kinematic range $2.0 < p_T < 18.0 \text{ GeV}/c$ and $2.20 < \eta < 4.75$, the production asymmetry is $A_P = (-0.96 \pm 0.26 \pm 0.18)\%$. The uncertainties quoted are statistical and systematic, respectively. The result assumes that any direct CP violation in the $D^+ \rightarrow K_S^0 \pi^+$ decay is negligible. No significant dependence on η or p_T is observed.

© 2012 CERN. Published by Elsevier B.V. All rights reserved.

1. Introduction

The Large Hadron Collider (LHC) offers an excellent opportunity to study heavy flavour physics. The rate of production of $c\bar{c}$ and $b\bar{b}$ pairs is substantial in the forward region close to the beam direction. The associated cross-sections were measured at the LHCb experiment in the forward region to be $\sigma_{c\bar{c}} = 1230 \pm 190 \mu\text{b}$ and $\sigma_{b\bar{b}} = 74 \pm 14 \mu\text{b}$ at $\sqrt{s} = 7 \text{ TeV}$ [1,2].

Direct production of $c\bar{c}$ pairs at the LHC occurs almost entirely via QCD and electroweak processes that do not discriminate between c and \bar{c} quarks. However, in hadronization the symmetry is broken by the presence of valence quarks, which introduce several processes that distinguish between c and \bar{c} quarks [3–5]. For example, a c quark could couple to valence quarks to form a charmed baryon, leaving an excess of \bar{c} quarks. These would hadronize to create an excess of D^- mesons over D^+ mesons. Furthermore, the kinematic distributions of charmed hadrons and their antiparticles can differ, introducing production asymmetries in local kinematic regions. Analogous production asymmetries in the strange sector are well-established at the LHC, and are seen to be large at high rapidity [6]. However, no evidence for a D_s^+ production asymmetry was found in a recent study [7].

Searches for CP violation (CPV) in charmed hadron decays can be used to probe for evidence of physics beyond the Standard Model [8]. Direct CPV is measured using time-integrated observables, and is of particular interest following evidence for CPV in

two-body D^0 decays reported by LHCb [9] and subsequently by CDF [10]. In order to understand the origin of this effect, more precise measurements of CP asymmetries in a suite of decay modes are required. Production asymmetries have the same experimental signature as direct CPV effects and are potentially much larger than the CP asymmetries to be determined. This problem can sometimes be avoided by taking the difference in asymmetry between two decay modes with a common production asymmetry [9] or by studying the difference in kinematic distributions of multi-body decays [11]. However, these methods result in a reduction in statistical power and are not applicable to all final states. It is therefore important to measure production asymmetries directly.

In this Letter, the D^\pm production asymmetry, defined as

$$A_P = \frac{\sigma(D^+) - \sigma(D^-)}{\sigma(D^+) + \sigma(D^-)}, \quad (1)$$

for cross-sections $\sigma(D^\pm)$, is determined with a sample of $D^+ \rightarrow K_S^0 \pi^+$, $K_S^0 \rightarrow \pi^+ \pi^-$ decays.¹ As there are no charged kaons in the final state, the detector biases in this decay are simpler to understand than those in other D^+ decays with higher branching fractions. The K_S^0 , a pseudoscalar particle, has a charge-symmetric decay, and the charge asymmetry in the pion efficiency at LHCb has been measured previously for the 2011 data sample [7]. However, there is the possibility of CPV in the decay. The expected CPV in the D^+ decay, due to the interference of the Cabibbo-favoured

[☆] © CERN for the benefit of the LHCb Collaboration.

¹ Charge conjugate decays are implied throughout this Letter unless stated otherwise.

and doubly Cabibbo-suppressed amplitudes, is defined by the charge asymmetry in the partial widths $\Gamma(D^\pm)$,

$$A_{CP} = \frac{\Gamma(D^+) - \Gamma(D^-)}{\Gamma(D^+) + \Gamma(D^-)}. \quad (2)$$

A_{CP} is negligible in the Standard Model: a simple consideration of the CKM matrix leads to a value of at most 1×10^{-4} depending on the strong phase difference between the two amplitudes [12]. Since both amplitudes are at tree level, no enhancement of CPV due to new physics is expected. The current world-best measurement of A_{CP} , by the Belle Collaboration, is consistent with zero: $(0.024 \pm 0.094 \pm 0.067)\%$ [13]. On the other hand, CPV in the neutral kaon system induces an asymmetry which must be considered. This will be discussed further in Section 5.

2. Detector description

The LHCb detector [14] is a single-arm forward spectrometer covering the pseudorapidity range $2 < \eta < 5$, designed for the study of particles containing b or c quarks. The detector includes a high precision tracking system consisting of a silicon-strip vertex detector (VELO) surrounding the pp interaction region, a large-area silicon-strip detector located upstream of a dipole magnet of reversible polarity with a bending power of about 4 Tm, and three stations of silicon-strip detectors and straw drift-tubes placed downstream. The combined tracking system has a momentum resolution $\Delta p/p$ that varies from 0.4% at 5 GeV/c to 0.6% at 100 GeV/c, and an impact parameter (IP) resolution of 20 μm for tracks with high transverse momentum p_T . Charged hadrons are identified using two ring-imaging Cherenkov detectors. Photon, electron and hadron candidates are identified by a calorimeter system consisting of scintillating-pad and pre-shower detectors, an electromagnetic calorimeter and a hadronic calorimeter. Muons are identified by a system composed of alternating layers of iron and multiwire proportional chambers. The trigger consists of a hardware stage, based on information from the calorimeter and muon systems, an inclusive software stage, which uses the tracking system, and a second software stage that exploits the full event information.

3. Dataset and selection

The data sample used in this analysis corresponds to 1.0 fb^{-1} of pp collisions taken at a centre of mass energy of 7 TeV at the Large Hadron Collider in 2011. The polarity of the LHCb magnetic field was changed several times during the run, and approximately half of the data were taken with each polarity, referred to as ‘magnet-up’ and ‘magnet-down’ data hereafter. To optimise the event selection and estimate efficiencies, 12.5 million pp collision events containing $D^+ \rightarrow K_S^0 \pi^+$, $K_S^0 \rightarrow \pi^- \pi^+$ decays were simulated with PYTHIA 6.4 [15] with a specific LHCb configuration [16]. Decays of hadronic particles are described by EVTGEN [17]. The interactions of the generated particles with the detector and its response are implemented using the GEANT4 toolkit [18] as described in Ref. [19].

Pairs of oppositely charged tracks with a pion mass hypothesis are combined to form K_S^0 candidates. Only those K_S^0 candidates with $p_T > 700 \text{ MeV}/c$ and invariant mass within 35 MeV/c^2 of the nominal value [20] are retained. Surviving candidates are then combined with a third charged track, the bachelor pion, to form a D^+ candidate, with the mass of the K_S^0 candidate constrained to its nominal value in a kinematic fit. Each of the three pion tracks must be detected in the VELO, so only those K_S^0 mesons that decay well within the VELO are used. This creates a bias towards short

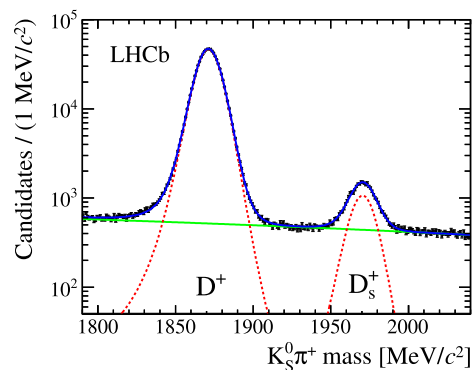


Fig. 1. Mass distribution of selected $K_S^0 \pi^+$ candidates. The data are represented by symbols with error bars. The dashed curves indicate the signal and the $D_s^+ \rightarrow K_S^0 \pi^+$ decays, the lower solid line represents the background shape, and the upper solid line shows the sum of all fit components.

K_S^0 decay times. Both the K_S^0 and D^+ candidates are required to have acceptable vertex fit quality.

Further requirements are applied in order to reduce the background and to align the selection of bachelor pions with the dataset used to determine the charge asymmetry in the tracking efficiency (see Section 6). The daughters of the K_S^0 must have $p > 2 \text{ GeV}/c$ and $p_T > 250 \text{ MeV}/c$. Impact parameter requirements are used to ensure that both the K_S^0 candidate and its daughter tracks do not originate at any primary vertex (PV) in the event, and the K_S^0 decay vertex must be at least 10 mm downstream of the PV with which it is associated. The bachelor pion must have $p > 5 \text{ GeV}/c$ and $p_T > 500 \text{ MeV}/c$, be positively identified as a pion rather than as a kaon, electron or muon, and must not come from any PV. In addition, fiducial requirements are applied as in Ref. [9] to exclude regions with large tracking efficiency asymmetry. All three tracks must have an acceptable track fit quality. The D^+ candidate is required to have $p_T > 1 \text{ GeV}/c$, to point to a PV (suppressing D from B decays), and to have a decay time significantly greater than zero. After these criteria are applied, the remaining background is mostly from random combinations of tracks. The invariant mass distribution of selected candidates is shown in Fig. 1.

In selected events, a trigger decision may be based on part or all of the D^+ signal candidate, on other particles in the event, or both. The second stage of the software trigger is required to find a fully reconstructed candidate which meets the criteria to be a signal $D^+ \rightarrow K_S^0 \pi^+$ decay. To control potential charge asymmetries introduced by the hardware trigger, two possibilities, not mutually exclusive, are allowed. The hardware trigger decision must be based on one or both of the K_S^0 daughter tracks, or on a particle other than the decay products of the D^+ candidate. In both cases, the inclusive software trigger must make a decision based on one of the three tracks that form the D^+ . For the first case, it is explicitly required that the same track activated the hardware trigger, and therefore this is independent of the D^+ charge. The second possibility does not depend directly on the D^+ charge, but an indirect dependence could be introduced if the probability for particles produced in association with the signal candidate to activate the trigger differs between D^+ and D^- . This will be discussed further in Section 7. After applying the selection and trigger requirements, 1,031,068 $K_S^0 \pi^+$ candidates remain.

4. Yield determination

The signal yields are measured in 48 bins of p_T and η using binned likelihood fits to the distribution of the $K_S^0 \pi^+$ mass m . The

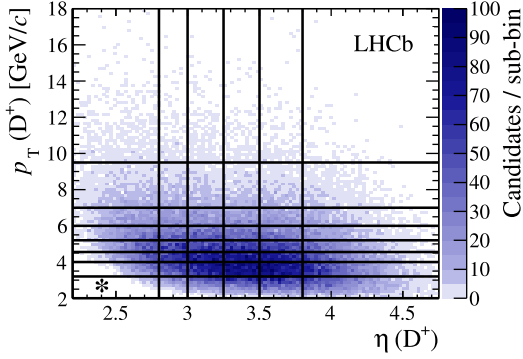


Fig. 2. Background-subtracted distribution of transverse momenta p_T versus pseudorapidity η for selected $D^+ \rightarrow K_S^0 \pi^+$ candidates in a signal region of $1845 < m < 1890$ MeV/ c^2 . The bin marked with an asterisk is excluded from the weighted average over the production asymmetries in the bins used to obtain the final result.

bins are shown in Fig. 2. The shapes of the $D_{(s)}^+ \rightarrow K_S^0 \pi^+$ mass peaks are described by ‘Cruiff’ functions [21],

$$f(m) \propto \exp\left(\frac{-(m - \mu)^2}{2\sigma_{L,R}^2 + (m - \mu)^2\alpha_{L,R}}\right) \quad (3)$$

with the measured masses defined by the free parameter μ , the widths by σ_L and σ_R , and the tails by α_L and α_R . The parameters α_L and σ_L are used for $m < \mu$ and α_R and σ_R for $m > \mu$. The background is fitted with a straight line plus an additional Gaussian component to account for background from $D_s^+ \rightarrow K_S^0 \pi^+ \pi^0$ decays. The yield of the latter is consistent with zero in most p_T , η bins. The fit is performed simultaneously over four subsamples (D^+ magnet-up, D^+ magnet-down, D^- magnet-up, and D^- magnet-down data) with the masses and yields of the $D_{(s)}^\pm$, and the yield of background, allowed to vary independently in the four subsamples. All other parameters are shared. The charge asymmetries are then determined from the yields. The results are cross-checked with a sideband subtraction procedure under the assumption of a linear background.

5. Effect of CP violation in the neutral kaon system

CP violation in the neutral kaon system can affect the observed asymmetry in the $D^+ \rightarrow K_S^0 \pi^+$ decay [22]. The bias on A_P due to the CPV depends on the decay time acceptance $F(t)$ of the K_S^0 meson, according to

$$A_\epsilon \sim 2\Re(\epsilon) \times \left[1 - \frac{\int_0^\infty F(t) e^{-\frac{1}{2}(\Gamma_S + \Gamma_L)t} (\cos \Delta m t - \frac{\Im(\epsilon)}{\Re(\epsilon)} \sin \Delta m t) dt}{\int_0^\infty F(t) e^{-\Gamma_S t} dt} \right], \quad (4)$$

where ϵ parameterises the indirect CPV in neutral kaon mixing, Γ_S and Γ_L are the decay widths of the K_S^0 and K_L^0 respectively, and Δm is their mass difference [23,24]. Direct CPV and terms of order ϵ^2 are neglected. To determine the decay time acceptance, the K_S^0 decay time is fitted with an empirical function shown in Fig. 3. All of the K_S^0 candidates used in this analysis decay inside the VELO with an average measured lifetime of 6.97 ± 0.02 ps, which is much shorter than the nominal K_S^0 lifetime of 89.5 ps. Using $\Re(\epsilon) = 1.65 \times 10^{-3}$ [20] in Eq. (4), we obtain $A_\epsilon = (2.831_{-0.004}^{+0.003}) \times 10^{-4}$ for the CPV in the neutral kaon system, where the uncertainty quoted is statistical only. This value is

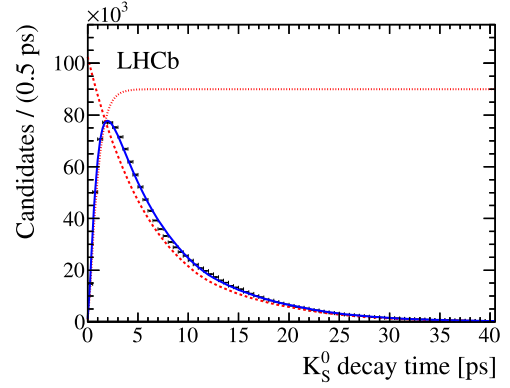


Fig. 3. Observed K_S^0 decay time distribution within the LHCb acceptance. The data points are fitted with an empirical function (solid curve). This contains a component for the upper decay time acceptance, due mainly to the requirement that the K_S^0 decays inside the VELO (dashed curve) and a component for the lower decay time acceptance, due to the selection cuts (dotted curve). These are shown scaled by arbitrary factors. The CPV is not sensitive to the fine details of the distribution, so the fit quality is not important.

subtracted from the measured production asymmetry and a systematic uncertainty equal to its central value is assigned.

6. Results

In order to convert the measured charge asymmetries in the 48 bins of p_T and η into production asymmetries, a correction for the asymmetry in the pion reconstruction efficiency is made. This asymmetry was evaluated previously in eight bins of pion azimuthal angle ϕ and two bins of pion momentum with a control sample of $D^{*+} \rightarrow D^0 \pi^+$, $D^0 \rightarrow K^- \pi^+ \pi^- \pi^+$ decays in the same dataset [7]. The average efficiency asymmetry ratios $\epsilon_{\pi^+}/\epsilon_{\pi^-}$ in that sample were found to be 0.9914 ± 0.0040 for magnet-up data and 1.0045 ± 0.0034 for magnet-down data.

After the correction is applied, the resulting asymmetries for magnet-up and magnet-down data in each D^+ p_T and η bin are averaged with equal weights to obtain the production asymmetries in two-dimensional bins of p_T and η , given in Table 1. Any left–right asymmetries that differ between the signal $D^+ \rightarrow K_S^0 \pi^+$ decay and the $D^0 \rightarrow K^- \pi^+ \pi^- \pi^+$ control channel will cancel in this average.

Reconstruction and selection efficiencies from the simulation are used to calculate binned efficiency-corrected yields. These are used to weight the production asymmetries in the average over the p_T and η bins. The result is an asymmetry for D^+ produced in the LHCb acceptance. The same weighting technique is applied to obtain production asymmetries as one-dimensional functions of p_T and η . The bin marked with an asterisk in Fig. 2 has a high cross-section but is mostly outside the acceptance and so it is excluded from the average. After subtracting the contribution from CPV in the kaon system, the production asymmetry is $(-0.96 \pm 0.19 \pm 0.18)\%$. The uncertainties are the statistical errors on the $D^+ \rightarrow K_S^0 \pi^+$ yields and that due to the tagged $D^0 \rightarrow K^- \pi^+ \pi^- \pi^+$ sample used to calculate the pion efficiencies. Summing these in quadrature, we obtain

$$A_P = (-0.96 \pm 0.26 \text{ (stat.)})\%.$$

The production asymmetry as a function of p_T and η is given in Fig. 4. No significant dependence of the asymmetry on these variables is observed. As a cross-check, the average production asymmetry is calculated for magnet-up and magnet-down data

Table 1

Production asymmetry for D^+ mesons, in percent, in (p_T, η) bins, for $2.0 < p_T < 18.0$ GeV/c and $2.20 < \eta < 4.75$. The uncertainties shown are statistical only; the systematic uncertainty is 0.17% (see Table 2).

p_T (GeV/c)	η					
	(2.20, 2.80)	(2.80, 3.00)	(3.00, 3.25)	(3.25, 3.50)	(3.50, 3.80)	(3.80, 4.75)
(2.00, 3.20)	-0.0 ± 2.5	-2.2 ± 1.2	-0.4 ± 0.8	-0.4 ± 0.7	-1.2 ± 0.6	-1.2 ± 0.5
(3.20, 4.00)	-0.4 ± 0.9	-0.4 ± 0.7	-0.4 ± 0.5	-1.1 ± 0.5	$+0.1 \pm 0.5$	-1.2 ± 0.5
(4.00, 4.55)	$+0.1 \pm 0.8$	-1.0 ± 0.8	-1.3 ± 0.6	-2.0 ± 0.6	-0.1 ± 0.6	-2.1 ± 0.7
(4.55, 5.20)	-1.6 ± 0.7	-0.6 ± 0.8	-0.5 ± 0.6	-0.7 ± 0.6	-1.6 ± 0.6	-2.0 ± 0.8
(5.20, 6.00)	-0.5 ± 0.7	-0.8 ± 0.8	$+0.2 \pm 0.7$	-0.3 ± 0.7	-0.6 ± 0.7	-1.2 ± 0.9
(6.00, 7.00)	-1.4 ± 0.8	$+0.5 \pm 1.0$	-0.9 ± 0.9	-0.6 ± 0.9	-0.7 ± 0.9	-1.6 ± 1.2
(7.00, 9.50)	-0.4 ± 0.8	-0.4 ± 1.1	-0.2 ± 1.1	$+1.7 \pm 1.1$	-1.4 ± 1.1	$+1.2 \pm 1.4$
(9.50, 18.00)	-0.6 ± 1.3	$+1.8 \pm 2.3$	-2.5 ± 2.2	$+1.8 \pm 2.4$	$+1.1 \pm 2.5$	-7 ± 11

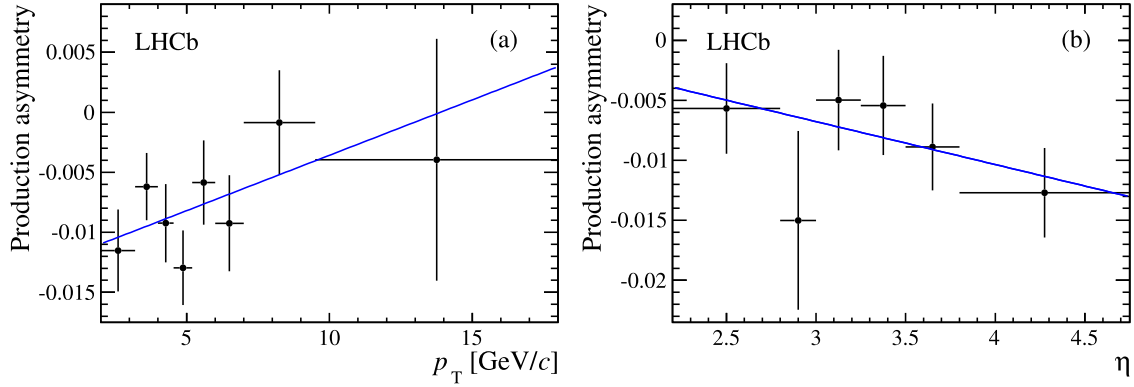


Fig. 4. Production asymmetry as a function of (a) transverse momentum p_T and (b) pseudorapidity η . The straight line fits have slopes of $(0.09 \pm 0.07) \times 10^{-2}$ (GeV/c) $^{-1}$ and $(-0.36 \pm 0.28)\%$, and values of χ^2 per degree of freedom of 5.5/6 and 2.2/4, respectively. The error bars include only the statistical uncertainty on the D^+ signal sample and are uncorrelated within a given plot.

Table 2

Summary of absolute values of systematic uncertainties on A_p . For the binned production asymmetries given in Table 1, all uncertainties except that on the reconstruction efficiency apply, giving a combined systematic uncertainty of 0.17%.

Systematic effect	Uncertainty (%)
Trigger asymmetries	0.15
D from B	0.04
Selection criteria	0.05
Running conditions	0.04
Pion efficiency	0.02
Fitting	0.04
Kaon CP violation	0.03
Weights (reconstruction efficiency)	0.05
Total including uncertainty on weights	0.18

separately, and found to be fully consistent: $(-1.07 \pm 0.41)\%$ and $(-0.85 \pm 0.34)\%$, respectively.

7. Systematic uncertainties

The sources of systematic uncertainty are summarised in Table 2. The dominant uncertainty of 1.5×10^{-3} is due to asymmetries introduced by the trigger. Events which are triggered independently of the signal decay, i.e. by a track that does not form part of the signal candidate, could be triggered by particles produced in association with the D^+ meson. If this occurs, the asymmetry in this sample would be correlated with the production asymmetry, and would bias the measurement of it. This was studied with a control sample of the abundant $D^+ \rightarrow K^-\pi^+\pi^+$ decay. To mimic the charge-unbiased sample of $D^+ \rightarrow K_S^0\pi^+$ decays which are triggered by a K_S^0 daughter, we choose the kaon and one pion at random and require that the trigger decision be based on one of these tracks. This is close to being charge-symmetric between D^+ and D^- candidates, with some residual effects due to

differences in material interaction between K^+ and K^- mesons. The raw asymmetry in this subsample of $D^+ \rightarrow K^-\pi^+\pi^+$ decays is then compared to that in the much larger sample of candidates that are triggered independently of the signal decay. The difference in raw charge asymmetry between these two samples, $(1.5 \pm 0.4) \times 10^{-3}$, is a measure of the scale of the bias. Unlike the signal, the $K^-\pi^+\pi^+$ decay also includes a component due to the K^+/K^- asymmetry, and therefore this is treated as a systematic uncertainty rather than a correction. This is cross-checked with other control samples such as $D_S^+ \rightarrow \phi\pi^+$ and the uncertainty is found to be conservative.

Further systematic uncertainties arise from the contamination of the prompt sample by D candidates that originate from B decays. The yield of these is calculated using the measured cross-sections [1,2], branching ratios, and efficiencies determined from the simulation. The fraction of D candidates from B decays is found to be $(1.2 \pm 0.3)\%$. This quantity is combined with the B^0 production asymmetry, which is estimated to be $(-1.0 \pm 1.3)\%$ [25], to determine the systematic uncertainty.

Certain selection criteria differ between the $D^+ \rightarrow K_S^0\pi^+$ signal sample and the $D^0 \rightarrow K^-\pi^+\pi^-\pi^+$ decays used to determine the asymmetry in the pion efficiencies. The charge asymmetry is found to depend weakly on the value of the requirement on the pion p_T . Pions in the signal sample must have $p_T > 500$ MeV/c while those in the control sample must have $p_T > 300$ MeV/c. A systematic uncertainty is calculated by estimating the proportion of signal candidates with $300 < p_T < 500$ MeV/c and multiplying this fraction by the difference between the charge asymmetries in the low p_T region and the average.

The difference in signal yields per pb^{-1} of integrated luminosity between magnet-up and magnet-down data is used to determine a systematic uncertainty for changes in running conditions that could impair the cancellation of detector asymmetries achieved

by averaging over the magnet polarities. There is also a systematic uncertainty on the pion efficiency asymmetry associated with the determination of the yields of $D^0 \rightarrow K^- \pi^+ \pi^- \pi^+$ decays. The error associated with the mass fit is determined by comparing fitted and sideband-subtracted results. The CPV in the neutral kaon decay, discussed in Section 5, is also included as a systematic uncertainty.

Other systematic effects such as regeneration in the neutral kaon system [26], second order effects due to the kinematic binning of the $D^+ \rightarrow K_S^0 \pi^+$ sample, and asymmetric backgrounds such as that from $D_s^+ \rightarrow K_S^0 K^+$ with the kaon misidentified as a pion, were considered but found to be negligible. When taking the average asymmetry weighted by the efficiency-corrected yield in each bin, the limited number of simulated events leads to an uncertainty on the reconstruction efficiency and hence on the per-bin weights. This does not contribute to the uncertainty on the individual asymmetries given in Table 1, which are calculated without using the simulation. A quadratic sum yields an overall systematic uncertainty of 1.8×10^{-3} .

In principle, CPV in the charm decay could occur via the interference of Cabibbo-favoured and doubly Cabibbo-suppressed amplitudes, but this is strongly suppressed by the CKM matrix and no evidence for it has been observed at the B -factories [27,13]. If we allowed for the possibility of new physics or large unexpected enhancements of the Standard Model CPV in these tree-level D^+ decays, the uncertainty on the null result found at Belle [13] would increase the total systematic uncertainty to 2.1×10^{-3} .

8. Conclusions

Evidence for a charge asymmetry in the production of D^+ mesons is observed at LHCb. In the kinematic range $2.0 < p_T < 18.0$ GeV/ c and $2.20 < \eta < 4.75$, excluding the region with $2.0 < p_T < 3.2$ GeV/ c , $2.20 < \eta < 2.80$, the average asymmetry is

$$A_P = (-0.96 \pm 0.26 \pm 0.18)\%$$

where the first uncertainty is statistical and the second is systematic. The result is inconsistent with zero at approximately three standard deviations. There is no evidence for a significant dependence on p_T or pseudorapidity at the present level of precision. The bias on the measured asymmetry due to CP violation in kaon decays has been calculated and found to be almost negligible for this dataset. These results are consistent with expectations [5] and lay the foundations for searches for CP violation in Cabibbo suppressed D^+ decays.

Acknowledgements

We express our gratitude to our colleagues in the CERN accelerator departments for the excellent performance of the LHC. We thank the technical and administrative staff at the LHCb institutes. We acknowledge support from CERN and from the national agencies: CAPES, CNPq, FAPERJ and FINEP (Brazil); NSFC (China); CNRS/IN2P3 and Region Auvergne (France); BMBF, DFG, HGF and MPG (Germany); SFI (Ireland); INFN (Italy); FOM and NWO (The Netherlands); SCSR (Poland); ANCS/IFA (Romania); MinES, Rosatom, RFBR and NRC “Kurchatov Institute” (Russia); MinECo,

XuntaGal and GENCAT (Spain); SNSF and SER (Switzerland); NAS Ukraine (Ukraine); STFC (United Kingdom); NSF (USA). We also acknowledge the support received from the ERC under FP7. The Tier1 computing centres are supported by IN2P3 (France), KIT and BMBF (Germany), INFN (Italy), NWO and SURF (The Netherlands), CIEMAT, IFAE and UAB (Spain), GridPP (United Kingdom). We are thankful for the computing resources put at our disposal by Yandex LLC (Russia), as well as to the communities behind the multiple open source software packages that we depend on.

Open access

This article is published Open Access at sciencedirect.com. It is distributed under the terms of the Creative Commons Attribution License 3.0, which permits unrestricted use, distribution, and reproduction in any medium, provided the original authors and source are credited.

References

- [1] R. Aaij, et al., Prompt charm production in pp collisions at $\sqrt{s} = 7$ TeV, LHCb-CONF-2010-013.
- [2] LHCb Collaboration, R. Aaij, et al., Phys. Lett. B 694 (2010) 209, arXiv:1009.2731.
- [3] E. Norrbin, Heavy quark production asymmetries, arXiv:hep-ph/9909437.
- [4] E. Norrbin, R. Vogt, Bottom production asymmetries at the LHC, in: Proceedings of the CERN 1999 Workshop on SM Physics (and More) at the LHC, arXiv:hep-ph/0003056.
- [5] E. Norrbin, T. Sjöstrand, Eur. Phys. J. C 17 (2000) 137, arXiv:hep-ph/0005110.
- [6] LHCb Collaboration, R. Aaij, et al., JHEP 1108 (2011) 034, arXiv:1107.0882.
- [7] LHCb Collaboration, R. Aaij, et al., Phys. Lett. B 713 (2012) 186, arXiv:1205.0897.
- [8] Y. Grossman, A.L. Kagan, Y. Nir, Phys. Rev. D 75 (2007) 036008, arXiv:hep-ph/0609178.
- [9] LHCb Collaboration, R. Aaij, et al., Phys. Rev. Lett. 108 (2012) 111602, arXiv:1112.0938.
- [10] CDF Collaboration, T. Aaltonen, et al., Phys. Rev. Lett. 109 (2012) 111801, arXiv:1207.2158.
- [11] LHCb Collaboration, R. Aaij, et al., Phys. Rev. D 84 (2011) 112008, arXiv:1110.3970.
- [12] I.I. Bigi, H. Yamamoto, Phys. Lett. B 349 (1995) 363, arXiv:hep-ph/9502238.
- [13] Belle Collaboration, B. Ko, et al., Phys. Rev. Lett. 109 (2012) 021601, arXiv:1203.6409; Belle Collaboration, B. Ko, et al., Phys. Rev. Lett. 109 (2012) 119903 (Erratum).
- [14] LHCb Collaboration, A.A. Alves Jr., et al., JINST 3 (2008) S08005.
- [15] T. Sjöstrand, S. Mrenna, P. Skands, JHEP 0605 (2006) 026, arXiv:hep-ph/0603175.
- [16] I. Belyaev, et al., in: Nuclear Science Symposium Conference Record (NSS/MIC), IEEE, 2010, p. 1155.
- [17] D.J. Lange, Nucl. Instrum. Meth. A 462 (2001) 152.
- [18] GEANT4 Collaboration, J. Allison, et al., IEEE Trans. Nucl. Sci. 53 (2006) 270; GEANT4 Collaboration, S. Agostinelli, et al., Nucl. Instrum. Meth. A 506 (2003) 250.
- [19] M. Clemencic, et al., J. Phys.: Conf. Ser. 331 (2011) 032023.
- [20] Particle Data Group, J. Beringer, et al., Phys. Rev. D 86 (2012) 010001.
- [21] BaBar Collaboration, P. del Amo Sanchez, et al., Phys. Rev. D 82 (2010) 051101, arXiv:1005.4087.
- [22] S. Bianco, F. Fabbri, D. Benson, I. Bigi, Riv. Nuovo Cim. 26 (7) (2003) 1, arXiv:hep-ex/0309021.
- [23] Y. Grossman, Y. Nir, JHEP 1204 (2012) 002, arXiv:1110.3790.
- [24] CPLEAR Collaboration, A. Apostolakis, et al., Eur. Phys. J. C 18 (2000) 41.
- [25] LHCb Collaboration, R. Aaij, et al., Phys. Rev. Lett. 108 (2012) 201601, arXiv:1202.6251.
- [26] J. Roehrig, et al., Phys. Rev. Lett. 38 (1977) 1116.
- [27] BaBar Collaboration, P. del Amo Sanchez, et al., Phys. Rev. D 83 (2011) 071103, arXiv:1011.5477.

LHCb Collaboration

R. Aaij³⁸, C. Abellan Beteta^{33,n}, A. Adametz¹¹, B. Adeva³⁴, M. Adinolfi⁴³, C. Adrover⁶, A. Affolder⁴⁹, Z. Ajaltouni⁵, J. Albrecht³⁵, F. Alessio³⁵, M. Alexander⁴⁸, S. Ali³⁸, G. Alkhazov²⁷, P. Alvarez Cartelle³⁴,

A.A. Alves Jr.²², S. Amato², Y. Amhis³⁶, L. Anderlini^{17,f}, J. Anderson³⁷, R.B. Appleby⁵¹,
 O. Aquines Gutierrez¹⁰, F. Archilli^{18,35}, A. Artamonov³², M. Artuso⁵³, E. Aslanides⁶, G. Auremma^{22,m},
 S. Bachmann¹¹, J.J. Back⁴⁵, C. Baesso⁵⁴, W. Baldini¹⁶, R.J. Barlow⁵¹, C. Barschel³⁵, S. Barsuk⁷,
 W. Barter⁴⁴, A. Bates⁴⁸, Th. Bauer³⁸, A. Bay³⁶, J. Beddow⁴⁸, I. Bediaga¹, S. Belogurov²⁸, K. Belous³²,
 I. Belyaev²⁸, E. Ben-Haim⁸, M. Benayoun⁸, G. Bencivenni¹⁸, S. Benson⁴⁷, J. Benton⁴³, A. Berezhnoy²⁹,
 R. Bernet³⁷, M.-O. Bettler⁴⁴, M. van Beuzekom³⁸, A. Bien¹¹, S. Bifani¹², T. Bird⁵¹, A. Bizzeti^{17,h},
 P.M. Bjørnstad⁵¹, T. Blake³⁵, F. Blanc³⁶, C. Blanks⁵⁰, J. Blouw¹¹, S. Blusk⁵³, A. Bobrov³¹, V. Bocci²²,
 A. Bondar³¹, N. Bondar²⁷, W. Bonivento¹⁵, S. Borghi^{48,51}, A. Borgia⁵³, T.J.V. Bowcock⁴⁹, C. Bozzi¹⁶,
 T. Brambach⁹, J. van den Brand³⁹, J. Bressieux³⁶, D. Brett⁵¹, M. Britsch¹⁰, T. Britton⁵³, N.H. Brook⁴³,
 H. Brown⁴⁹, A. Büchler-Germann³⁷, I. Burducea²⁶, A. Bursche³⁷, J. Buytaert³⁵, S. Cadeddu¹⁵, O. Callot⁷,
 M. Calvi^{20,j}, M. Calvo Gomez^{33,n}, A. Camboni³³, P. Campana^{18,35}, A. Carbone^{14,c}, G. Carbone^{21,k},
 R. Cardinale^{19,i}, A. Cardini¹⁵, H. Carranza-Mejia⁴⁷, L. Carson⁵⁰, K. Carvalho Akiba², G. Casse⁴⁹,
 M. Cattaneo³⁵, Ch. Cauet⁹, M. Charles⁵², Ph. Charpentier³⁵, P. Chen^{3,36}, N. Chiapolini³⁷,
 M. Chrzaszcz²³, K. Ciba³⁵, X. Cid Vidal³⁴, G. Ciezarek⁵⁰, P.E.L. Clarke⁴⁷, M. Clemencic³⁵, H.V. Cliff⁴⁴,
 J. Closier³⁵, C. Coca²⁶, V. Coco³⁸, J. Cogan⁶, E. Cogneras⁵, P. Collins³⁵, A. Comerma-Montells³³,
 A. Contu^{52,15}, A. Cook⁴³, M. Coombes⁴³, G. Corti³⁵, B. Couturier³⁵, G.A. Cowan³⁶, D. Craik⁴⁵,
 S. Cunliffe⁵⁰, R. Currie⁴⁷, C. D'Ambrosio³⁵, P. David⁸, P.N.Y. David³⁸, I. De Bonis⁴, K. De Bruyn³⁸,
 S. De Capua⁵¹, M. De Cian³⁷, J.M. De Miranda¹, L. De Paula², P. De Simone¹⁸, D. Decamp⁴,
 M. Deckenhoff⁹, H. Degaudenzi^{36,35}, L. Del Buono⁸, C. Deplano¹⁵, D. Derkach¹⁴, O. Deschamps⁵,
 F. Dettori³⁹, A. Di Canto¹¹, J. Dickens⁴⁴, H. Dijkstra³⁵, P. Diniz Batista¹, M. Dogaru²⁶,
 F. Domingo Bonal^{33,n}, S. Donleavy⁴⁹, F. Dordei¹¹, A. Dosil Suárez³⁴, D. Dossett⁴⁵, A. Dovbnya⁴⁰,
 F. Dupertuis³⁶, R. Dzhelyadin³², A. Dziurda²³, A. Dzyuba²⁷, S. Easo^{46,35}, U. Egede⁵⁰, V. Egorychev²⁸,
 S. Eidelman³¹, D. van Eijk³⁸, S. Eisenhardt⁴⁷, R. Ekelhof⁹, L. Eklund⁴⁸, I. El Rifai⁵, Ch. Elsasser³⁷,
 D. Elsby⁴², A. Falabella^{14,e}, C. Färber¹¹, G. Fardell⁴⁷, C. Farinelli³⁸, S. Farry¹², V. Fave³⁶,
 V. Fernandez Albor³⁴, F. Ferreira Rodrigues¹, M. Ferro-Luzzi³⁵, S. Filippov³⁰, C. Fitzpatrick³⁵,
 M. Fontana¹⁰, F. Fontanelli^{19,i}, R. Forty³⁵, O. Francisco², M. Frank³⁵, C. Frei³⁵, M. Frosini^{17,f},
 S. Furcas²⁰, A. Gallas Torreira³⁴, D. Galli^{14,c}, M. Gandelman², P. Gandini⁵², Y. Gao³, J.-C. Garnier³⁵,
 J. Garofoli⁵³, P. Garosi⁵¹, J. Garra Tico⁴⁴, L. Garrido³³, C. Gaspar³⁵, R. Gauld⁵², E. Gersabeck¹¹,
 M. Gersabeck³⁵, T. Gershon^{45,35}, Ph. Ghez⁴, V. Gibson⁴⁴, V.V. Gligorov³⁵, C. Göbel⁵⁴, D. Golubkov²⁸,
 A. Golutvin^{50,28,35}, A. Gomes², H. Gordon^{52,*}, M. Grabalosa Gándara³³, R. Graciani Diaz³³,
 L.A. Granado Cardoso³⁵, E. Graugés³³, G. Graziani¹⁷, A. Grecu²⁶, E. Greening⁵², S. Gregson⁴⁴,
 O. Grünberg⁵⁵, B. Gui⁵³, E. Gushchin³⁰, Yu. Guz³², T. Gys³⁵, C. Hadjivasiliou⁵³, G. Haefeli³⁶, C. Haen³⁵,
 S.C. Haines⁴⁴, S. Hall⁵⁰, T. Hampson⁴³, S. Hansmann-Menzemer¹¹, N. Harnew⁵², S.T. Harnew⁴³,
 J. Harrison⁵¹, P.F. Harrison⁴⁵, T. Hartmann⁵⁵, J. He⁷, V. Heijne³⁸, K. Hennessy⁴⁹, P. Henrard⁵,
 J.A. Hernando Morata³⁴, E. van Herwijnen³⁵, E. Hicks⁴⁹, D. Hill⁵², M. Hoballah⁵, P. Hopchev⁴,
 W. Hulsbergen³⁸, P. Hunt⁵², T. Huse⁴⁹, N. Hussain⁵², D. Hutchcroft⁴⁹, D. Hynds⁴⁸, V. Iakovenko⁴¹,
 P. Ilten¹², J. Imong⁴³, R. Jacobsson³⁵, A. Jaeger¹¹, M. Jahjah Hussein⁵, E. Jans³⁸, F. Jansen³⁸, P. Jaton³⁶,
 B. Jean-Marie⁷, F. Jing³, M. John⁵², D. Johnson⁵², C.R. Jones⁴⁴, B. Jost³⁵, M. Kaballo⁹, S. Kandybei⁴⁰,
 M. Karacson³⁵, T.M. Karbach³⁵, I.R. Kenyon⁴², U. Kerzel³⁵, T. Ketel³⁹, A. Keune³⁶, B. Khanji²⁰,
 Y.M. Kim⁴⁷, O. Kochebina⁷, V. Komarov^{36,29}, R.F. Koopman³⁹, P. Koppenburg³⁸, M. Korolev²⁹,
 A. Kozlinskiy³⁸, L. Kravchuk³⁰, K. Kreplin¹¹, M. Kreps⁴⁵, G. Krocker¹¹, P. Krokovny³¹, F. Kruse⁹,
 M. Kucharczyk^{20,23,j}, V. Kudryavtsev³¹, T. Kvaratskheliya^{28,35}, V.N. La Thi³⁶, D. Lacarrere³⁵,
 G. Lafferty⁵¹, A. Lai¹⁵, D. Lambert⁴⁷, R.W. Lambert³⁹, E. Lanciotti³⁵, G. Lanfranchi^{18,35},
 C. Langenbruch³⁵, T. Latham⁴⁵, C. Lazzeroni⁴², R. Le Gac⁶, J. van Leerdam³⁸, J.-P. Lees⁴, R. Lefèvre⁵,
 A. Leflat^{29,35}, J. Lefrançois⁷, O. Leroy⁶, T. Lesiak²³, Y. Li³, L. Li Gioi⁵, M. Liles⁴⁹, R. Lindner³⁵, C. Linn¹¹,
 B. Liu³, G. Liu³⁵, J. von Loeben²⁰, J.H. Lopes², E. Lopez Asamar³³, N. Lopez-March³⁶, H. Lu³,
 J. Luisier³⁶, H. Luo⁴⁷, A. Mac Raighne⁴⁸, F. Machefert⁷, I.V. Machikhiliyan^{4,28}, F. Maciuc²⁶,
 O. Maev^{27,35}, J. Magnin¹, M. Maino²⁰, S. Malde⁵², G. Manca^{15,d}, G. Mancinelli⁶, N. Mangiafave⁴⁴,
 U. Marconi¹⁴, R. Märki³⁶, J. Marks¹¹, G. Martellotti²², A. Martens⁸, L. Martin⁵², A. Martín Sánchez⁷,
 M. Martinelli³⁸, D. Martinez Santos³⁵, D. Martins Tostes², A. Massafferri¹, R. Matev³⁵, Z. Mathe³⁵,
 C. Matteuzzi²⁰, M. Matveev²⁷, E. Maurice⁶, A. Mazurov^{16,30,35,e}, J. McCarthy⁴², G. McGregor⁵¹,
 R. McNulty¹², M. Meissner¹¹, M. Merk³⁸, J. Merkel⁹, D.A. Milanes¹³, M.-N. Minard⁴,

J. Molina Rodriguez⁵⁴, S. Monteil⁵, D. Moran⁵¹, P. Morawski²³, R. Mountain⁵³, I. Mous³⁸, F. Muheim⁴⁷, K. Müller³⁷, R. Muresan²⁶, B. Muryn²⁴, B. Muster³⁶, J. Mylroie-Smith⁴⁹, P. Naik⁴³, T. Nakada³⁶, R. Nandakumar⁴⁶, I. Nasteva¹, M. Needham⁴⁷, N. Neufeld³⁵, A.D. Nguyen³⁶, T.D. Nguyen³⁶, C. Nguyen-Mau^{36,o}, M. Nicol⁷, V. Niess⁵, N. Nikitin²⁹, T. Nikodem¹¹, A. Nomerotski^{52,35}, A. Novoselov³², A. Oblakowska-Mucha²⁴, V. Obraztsov³², S. Oggero³⁸, S. Ogilvy⁴⁸, O. Okhrimenko⁴¹, R. Oldeman^{15,35,d}, M. Orlandea²⁶, J.M. Otalora Goicochea², P. Owen⁵⁰, B.K. Pal⁵³, A. Palano^{13,b}, M. Palutan¹⁸, J. Panman³⁵, A. Papanestis⁴⁶, M. Pappagallo⁴⁸, C. Parkes⁵¹, C.J. Parkinson⁵⁰, G. Passaleva¹⁷, G.D. Patel⁴⁹, M. Patel⁵⁰, G.N. Patrick⁴⁶, C. Patrignani^{19,i}, C. Pavel-Nicorescu²⁶, A. Pazos Alvarez³⁴, A. Pellegrino³⁸, G. Penso^{22,l}, M. Pepe Altarelli³⁵, S. Perazzini^{14,c}, D.L. Perego^{20,j}, E. Perez Trigo³⁴, A. Pérez-Calero Yzquierdo³³, P. Perret⁵, M. Perrin-Terrin⁶, G. Pessina²⁰, K. Petridis⁵⁰, A. Petrolini^{19,i}, A. Phan⁵³, E. Picatoste Olloqui³³, B. Pie Valls³³, B. Pietrzyk⁴, T. Pilař⁴⁵, D. Pinci²², S. Playfer⁴⁷, M. Plo Casasus³⁴, F. Polci⁸, G. Polok²³, A. Poluektov^{45,31}, E. Polcarpo², D. Popov¹⁰, B. Popovici²⁶, C. Potterat³³, A. Powell⁵², J. Prisciandaro³⁶, V. Pugatch⁴¹, A. Puig Navarro³⁶, W. Qian⁴, J.H. Rademacker⁴³, B. Rakotomiamanana³⁶, M.S. Rangel², I. Raniuk⁴⁰, N. Rauschmayr³⁵, G. Raven³⁹, S. Redford⁵², M.M. Reid⁴⁵, A.C. dos Reis¹, S. Ricciardi⁴⁶, A. Richards⁵⁰, K. Rinnert⁴⁹, V. Rives Molina³³, D.A. Roa Romero⁵, P. Robbe⁷, E. Rodrigues^{48,51}, P. Rodriguez Perez³⁴, G.J. Rogers⁴⁴, S. Roiser³⁵, V. Romanovsky³², A. Romero Vidal³⁴, J. Rouvinet³⁶, T. Ruf³⁵, H. Ruiz³³, G. Sabatino^{22,k}, J.J. Saborido Silva³⁴, N. Sagidova²⁷, P. Sail⁴⁸, B. Saitta^{15,d}, C. Salzmann³⁷, B. Sanmartin Sedes³⁴, M. Sannino^{19,i}, R. Santacesaria²², C. Santamarina Rios³⁴, R. Santinelli³⁵, E. Santovetti^{21,k}, M. Sapunov⁶, A. Sarti^{18,l}, C. Satriano^{22,m}, A. Satta²¹, M. Savrie^{16,e}, P. Schaack⁵⁰, M. Schiller³⁹, H. Schindler³⁵, S. Schleich⁹, M. Schlupp⁹, M. Schmelling¹⁰, B. Schmidt³⁵, O. Schneider³⁶, A. Schopper³⁵, M.-H. Schune⁷, R. Schwemmer³⁵, B. Sciascia¹⁸, A. Sciubba^{18,l}, M. Seco³⁴, A. Semennikov²⁸, K. Senderowska²⁴, I. Sepp⁵⁰, N. Serra³⁷, J. Serrano⁶, P. Seyfert¹¹, M. Shapkin³², I. Shapoval^{40,35}, P. Shatalov²⁸, Y. Shcheglov²⁷, T. Shears^{49,35}, L. Shekhtman³¹, O. Shevchenko⁴⁰, V. Shevchenko²⁸, A. Shires⁵⁰, R. Silva Coutinho⁴⁵, T. Skwarnicki⁵³, N.A. Smith⁴⁹, E. Smith^{52,46}, M. Smith⁵¹, K. Sobczak⁵, F.J.P. Soler⁴⁸, F. Soomro^{18,35}, D. Souza⁴³, B. Souza De Paula², B. Spaan⁹, A. Sparkes⁴⁷, P. Spradlin⁴⁸, F. Stagni³⁵, S. Stahl¹¹, O. Steinkamp³⁷, S. Stoica²⁶, S. Stone⁵³, B. Storaci³⁸, M. Straticiu²⁶, U. Straumann³⁷, V.K. Subbiah³⁵, S. Swientek⁹, M. Szczekowski²⁵, P. Szczypka^{36,35}, T. Szumlak²⁴, S. T'Jampens⁴, M. Teklishyn⁷, E. Teodorescu²⁶, F. Teubert³⁵, C. Thomas⁵², E. Thomas³⁵, J. van Tilburg¹¹, V. Tisserand⁴, M. Tobin³⁷, S. Tolk³⁹, D. Tonelli³⁵, S. Topp-Joergensen⁵², N. Torr⁵², E. Tournefier^{4,50}, S. Tourneur³⁶, M.T. Tran³⁶, A. Tsaregorodtsev⁶, P. Tsoelas³⁸, N. Tuning³⁸, M. Ubeda Garcia³⁵, A. Ukleja²⁵, D. Urner⁵¹, U. Uwer¹¹, V. Vagnoni¹⁴, G. Valenti¹⁴, R. Vazquez Gomez³³, P. Vazquez Regueiro³⁴, S. Vecchi¹⁶, J.J. Velthuis⁴³, M. Veltri^{17,g}, G. Veneziano³⁶, M. Vesterinen³⁵, B. Viaud⁷, I. Videau⁷, D. Vieira², X. Vilasis-Cardona^{33,n}, J. Visniakov³⁴, A. Vollhardt³⁷, D. Volyanskyy¹⁰, D. Voong⁴³, A. Vorobyev²⁷, V. Vorobyev³¹, H. Voss¹⁰, C. Voß⁵⁵, R. Waldi⁵⁵, R. Wallace¹², S. Wandernoth¹¹, J. Wang⁵³, D.R. Ward⁴⁴, N.K. Watson⁴², A.D. Webber⁵¹, D. Websdale⁵⁰, M. Whitehead⁴⁵, J. Wicht³⁵, D. Wiedner¹¹, L. Wiggers³⁸, G. Wilkinson⁵², M.P. Williams^{45,46}, M. Williams^{50,p}, F.F. Wilson⁴⁶, J. Wishahi⁹, M. Witek²³, W. Witzeling³⁵, S.A. Wotton⁴⁴, S. Wright⁴⁴, S. Wu³, K. Wyllie³⁵, Y. Xie^{47,35}, F. Xing⁵², Z. Xing⁵³, Z. Yang³, R. Young⁴⁷, X. Yuan³, O. Yushchenko³², M. Zangoli¹⁴, M. Zavertyaev^{10,a}, F. Zhang³, L. Zhang⁵³, W.C. Zhang¹², Y. Zhang³, A. Zhelezov¹¹, L. Zhong³, A. Zvyagin³⁵

¹ Centro Brasileiro de Pesquisas Físicas (CBPF), Rio de Janeiro, Brazil

² Universidade Federal do Rio de Janeiro (UFRJ), Rio de Janeiro, Brazil

³ Center for High Energy Physics, Tsinghua University, Beijing, China

⁴ LAPP, Université de Savoie, CNRS/IN2P3, Annecy-Le-Vieux, France

⁵ Clermont Université, Université Blaise Pascal, CNRS/IN2P3, LPC, Clermont-Ferrand, France

⁶ CPPM, Aix-Marseille Université, CNRS/IN2P3, Marseille, France

⁷ LAL, Université Paris-Sud, CNRS/IN2P3, Orsay, France

⁸ LPNHE, Université Pierre et Marie Curie, Université Paris Diderot, CNRS/IN2P3, Paris, France

⁹ Fakultät Physik, Technische Universität Dortmund, Dortmund, Germany

¹⁰ Max-Planck-Institut für Kernphysik (MPIK), Heidelberg, Germany

¹¹ Physikalisches Institut, Ruprecht-Karls-Universität Heidelberg, Heidelberg, Germany

¹² School of Physics, University College Dublin, Dublin, Ireland

¹³ Sezione INFN di Bari, Bari, Italy

¹⁴ Sezione INFN di Bologna, Bologna, Italy

¹⁵ Sezione INFN di Cagliari, Cagliari, Italy

¹⁶ Sezione INFN di Ferrara, Ferrara, Italy

- ¹⁷ Sezione INFN di Firenze, Firenze, Italy
¹⁸ Laboratori Nazionali dell'INFN di Frascati, Frascati, Italy
¹⁹ Sezione INFN di Genova, Genova, Italy
²⁰ Sezione INFN di Milano Bicocca, Milano, Italy
²¹ Sezione INFN di Roma Tor Vergata, Roma, Italy
²² Sezione INFN di Roma La Sapienza, Roma, Italy
²³ Henryk Niewodniczanski Institute of Nuclear Physics Polish Academy of Sciences, Kraków, Poland
²⁴ AGH University of Science and Technology, Kraków, Poland
²⁵ National Center for Nuclear Research (NCBJ), Warsaw, Poland
²⁶ Horia Hulubei National Institute of Physics and Nuclear Engineering, Bucharest-Magurele, Romania
²⁷ Petersburg Nuclear Physics Institute (PNPI), Gatchina, Russia
²⁸ Institute of Theoretical and Experimental Physics (ITEP), Moscow, Russia
²⁹ Institute of Nuclear Physics, Moscow State University (SINP MSU), Moscow, Russia
³⁰ Institute for Nuclear Research of the Russian Academy of Sciences (INR RAN), Moscow, Russia
³¹ Budker Institute of Nuclear Physics (SB RAS) and Novosibirsk State University, Novosibirsk, Russia
³² Institute for High Energy Physics (IHEP), Protvino, Russia
³³ Universitat de Barcelona, Barcelona, Spain
³⁴ Universidad de Santiago de Compostela, Santiago de Compostela, Spain
³⁵ European Organization for Nuclear Research (CERN), Geneva, Switzerland
³⁶ Ecole Polytechnique Fédérale de Lausanne (EPFL), Lausanne, Switzerland
³⁷ Physik-Institut, Universität Zürich, Zürich, Switzerland
³⁸ Nikhef National Institute for Subatomic Physics, Amsterdam, The Netherlands
³⁹ Nikhef National Institute for Subatomic Physics and VU University Amsterdam, Amsterdam, The Netherlands
⁴⁰ NSC Kharkiv Institute of Physics and Technology (NSC KIPT), Kharkiv, Ukraine
⁴¹ Institute for Nuclear Research of the National Academy of Sciences (KINR), Kyiv, Ukraine
⁴² University of Birmingham, Birmingham, United Kingdom
⁴³ H.H. Wills Physics Laboratory, University of Bristol, Bristol, United Kingdom
⁴⁴ Cavendish Laboratory, University of Cambridge, Cambridge, United Kingdom
⁴⁵ Department of Physics, University of Warwick, Coventry, United Kingdom
⁴⁶ STFC Rutherford Appleton Laboratory, Didcot, United Kingdom
⁴⁷ School of Physics and Astronomy, University of Edinburgh, Edinburgh, United Kingdom
⁴⁸ School of Physics and Astronomy, University of Glasgow, Glasgow, United Kingdom
⁴⁹ Oliver Lodge Laboratory, University of Liverpool, Liverpool, United Kingdom
⁵⁰ Imperial College London, London, United Kingdom
⁵¹ School of Physics and Astronomy, University of Manchester, Manchester, United Kingdom
⁵² Department of Physics, University of Oxford, Oxford, United Kingdom
⁵³ Syracuse University, Syracuse, NY, United States
⁵⁴ Pontifícia Universidade Católica do Rio de Janeiro (PUC-Rio), Rio de Janeiro, Brazil^q
⁵⁵ Institut für Physik, Universität Rostock, Rostock, Germany^r

* Corresponding author.

E-mail address: hamish.gordon@cern.ch (H. Gordon).

^a P.N. Lebedev Physical Institute, Russian Academy of Science (LPI RAS), Moscow, Russia.

^b Università di Bari, Bari, Italy.

^c Università di Bologna, Bologna, Italy.

^d Università di Cagliari, Cagliari, Italy.

^e Università di Ferrara, Ferrara, Italy.

^f Università di Firenze, Firenze, Italy.

^g Università di Urbino, Urbino, Italy.

^h Università di Modena e Reggio Emilia, Modena, Italy.

ⁱ Università di Genova, Genova, Italy.

^j Università di Milano Bicocca, Milano, Italy.

^k Università di Roma Tor Vergata, Roma, Italy.

^l Università di Roma La Sapienza, Roma, Italy.

^m Università della Basilicata, Potenza, Italy.

ⁿ LIFAELS, La Salle, Universitat Ramon Llull, Barcelona, Spain.

^o Hanoi University of Science, Hanoi, Viet Nam.

^p Massachusetts Institute of Technology, Cambridge, MA, United States.

^q Associated to Universidade Federal do Rio de Janeiro (UFRJ), Rio de Janeiro, Brazil.

^r Associated to Physikalisches Institut, Ruprecht-Karls-Universität Heidelberg, Heidelberg, Germany.